2014

PC BASED ELECTROLYTES WITH LIDFOB AS AN ALTERNATIVE SALT FOR LITHIUM-ION BATTERIES

Brandon M. Knight
University of Rhode Island, bknight@chm.uri.edu

PC BASED ELECTROLYTES WITH LIDFOB AS AN ALTERNATIVE SALT FOR LITHIUM-ION BATTERIES

BY

BRANDON M. KNIGHT

A DISSERTATION SUBMITTED IN PARTIAL FULFILLMENT OF THE

REQUIREMENTS FOR THE DEGREE OF

DOCTOR OF PHILOSOPHY

IN

CHEMISTRY

UNIVERSITY OF RHODE ISLAND

2014

DOCTOR OF PHILOSOPHY DISSERTATION

OF

BRANDON M. KNIGHT

APPROVED:

Thesis Committee:

Major Professor Brett L. Lucht

William B. Euler

David R. Heskett

Nasser H. Zawia
DEAN OF THE GRADUATE SCHOOL

UNIVERSITY OF RHODE ISLAND
2014

ABSTRACT

Lithium-ion batteries (LIBs) have been greatly sought after as a source of renewable energy storage. LIBs have a wide range of applications including but not limited portable electronic devices, electric vehicles, and power tools. As a direct result of their commercial viability an insatiable hunger for knowledge, advancement within the field of LIBs has been omnipresent for the last two decades. However, there are set backs evident within the LIB field; most notably the limitations of standard electrolyte formulations and $LiPF_6$ lithium salt. The standard primary carbonate of ethylene carbonate (EC) has a very limited operating range due to its innate physical properties, and the $LiPF_6$ salt is known to readily decompose to form HF which can further degrade LIB longevity. The goal of our research is to explore the use of a new primary salt LiDFOB in conjunction with a propylene carbonate based electrolyte to establish a more flexible electrolyte formulation by constructing coin cells and cycling them under various conditions to give a clear understanding of each formulation inherent performance capabilities. Our studies show that 1.2M LiDFOB in 3:7 PC/EMC + 1.5% VC is capable of performing comparably to the standard 1.2M $LiPF_6$ in 3:7 EC/EMC at 25°C and the PC electrolyte also illustrates performance superior to the standard at 55°C.

The degradation of lithium manganese spinel electrodes, including $LiNi_{0.5}Mn_{1.5}O_4$, is an area of great concern within the field of lithium ion batteries (LIBs). Manganese containing cathode materials frequently have problems associated with Mn dissolution which significantly reduces the cycle life of LIB. Thus the stability of the cathode material is paramount to the performance of Mn spinel cathode

materials in LIBs. In an effort to gain a better understanding of the stability of $LiNi_{0.5}Mn_{1.5}O_4$ in common $LiPF_6$/carbonate electrolytes, samples were stored at elevated temperature in the presence of electrolyte. Then after storage both the electrolyte solution and uncharged cathode particles were analyzed. The solid cathode particles were analyzed via scanning electron microscopy (SEM) whereas the electrolyte solution was analyzed using inductively coupled plasma mass spectroscopy (ICP-MS). The SEM analysis assists with elucidation of changes to the surfaces of the cathode particles. The ICP-MS of the electrolyte allows the determination of the extent of Mn and Ni dissolution. Samples of $LiNi_{0.5}Mn_{1.5}O_4$ with different crystal surface facets were prepared to investigate the role of particle morphology in Mn and Ni dissolution. The factors affecting Mn and Ni dissolution and methods to inhibit dissolution will be discussed

ACKNOWLEDGMENTS

I would like to thank my research advisor Dr. Brett L. Lucht for the opportunity to conduct research within his laboratory as this achievement would not have been possible without his support. I would also like to thank Dr. Bill Euler, Dr. Susan Geldart, and the University of Rhode Island Department of Chemistry for their continued support and perseverance in even the darkest of days. Finally, I would like to thank Mr. Mike Platek at the University of Rhode Island's Department of Electrical Engineering for his technical expertise proved invaluable to my research over the years.

"The only true wisdom is in knowing that you know nothing."

-Socrates[1]

[1] English translation/interpretation of a quotation attributed to Socrates in Plato's *Apology*.

PREFACE

The dissertation is written in manuscript format in accordance with the University of Rhode Island Graduate School guidelines. The first chapter of this dissertation provides a brief introduction into lithium-ion batteries and the tradition co-solvents used within the electrolytes. The second, third, and fourth chapters are manuscripts that will be submitted to the Journal of Power Sources for publication.

TABLE OF CONTENTS

LIST OF TABLES

TABLE PAGE

LIST OF FIGURES

CHAPTER 1

INTRODUCTION

Background

The search for renewable energy sources has been motivated by the need for an alternative to our inherent reliance on fossil fuels which began in the wake of the Industrial Revolution. [1] Due to major complications with lithium metal batteries [2], lithium-ion batteries were sought after to fill the void left by their lithium metal predecessors due to their high gravimetric and volumetric energy densities. [3] Today, lithium-ion batteries are the main choice for many applications including (but not limited to) portable electronics (such as cellular phones), hybrid electric vehicles, electric vehicles, and aerospace applications. [4-6] The wide array of applications in conjunction with the omnipresent energy crisis facing the world furthers the demand for deeper understanding of mechanics involved in battery systems; understanding and how these systems affect all the major components of the lithium-ion battery will greatly augment the knowledge base of the within the field of renewable energy sources as a whole.

Lithium-ion batteries use lithium-ion intercalation mechanics in order to store charge within a particular battery cell. [3] In order to achieve proper intercalation mechanics very specific types of electrodes must be used. The cathode generally consists of a lithium metal oxide which functions as a source for lithium-ions. The anode is usually a graphitic type carbon which in turn can act as an acceptor for

lithium-ions. During a charge cycle, lithium-ions are removed from the cathode and intercalate in-between the graphene sheets of the anode. Conversely, during discharge the lithium-ions de-intercalate and traverse back to the cathode. Thus, the theoretical capacities of every lithium-ion cell are largely dependent on the physical properties of the materials used; ultimately the cathode's material will determine the maximum capacities that can be achieved. However, other primary components of the lithium-ion battery system also play a large role in the overall capacities that can be seen. [3]

The separator is a crucial structure within the lithium-ion battery cell. The separator is generally composed of a porous polyolefin that allows for ion transfer to and from the electrodes. The major purpose of the separator is to isolate both the cathode and the anode from each other in order to prevent an electrical short during cycling. Therefore it is important that the separator be thin and porous enough to limit ionic internal resistance (allowing for facile lithium-ion flow) but also be durable enough to prevent any deformation that might lead to the electrodes coming in contact with each other. Additionally, the separator must allow for the electrolyte and its' components to flow freely through the separator. Therefore, the assertion that the separator is a crucial component of the battery cell construction is irrefutable. However, as chemists, understanding the electrolyte itself is easily the most compelling aspect of the entire lithium-ion battery system.

The electrolyte is indubitably one of the most important components of the lithium-ion battery systems as its characteristics are multifaceted. The electrolyte facilitates lithium-ion flow through the entire system; without the electrolyte no ion transfer would occur. The electrolyte is usually composed ethylene carbonate and a

blend linear carbonates which in turn solvate the transferable lithium-ions from one electrode to the other. [3] In conjunction with the carbonates, an appropriate lithium metal salt (traditionally lithium hexafluorophosphate) is added to the carbonate blend in order to assist with the ion conductivity of the system in its entirety. The carbonates work to create a solvent sheath around transferable lithium-ions allowing them to flow freely from one electrode to the other. [2] Therefore, optimizing the conductivity and solubility (as well as other colligative properties) of the electrolyte are crucial to the overall performance and inherent kinetics of any lithium-ion battery system. Furthermore, the electrolyte also contributes to another inextricable component of the systems, the solid electrolyte interface.

The solid electrolyte interface (SEI) is pivotal to the overall functioning of any lithium-ion battery system. [7-8] During cycling, the electrolyte inevitably decomposes and the reduction products from the electrolyte composition are utilized in the formation of the SEI. Logically, due to the fact the SEI is composed of reduction products, the SEI forms primarily on the surface of the anode. The SEI acts as a passivation layer that allows for ion transfer through the SEI to the electrode as well as working to protect the electrolyte from continual decomposition. [7-8] The SEI acting as a passivation layer protects against further electrolyte reduction on the surface which in turn helps to extend the overall life of the electrolyte and by association the life of the battery itself. Therefore, understanding the SEI and especially what helps to create a stable SEI is an incredibly powerful force to wield within the realm of lithium-ion batteries and thus should not be ignore but rather embraced. Due to the enticing possibilities that exist in understanding the SEI, it is the major aspect of our research.

PC and LiDFOB Incorporation into the Electrolyte

Propylene carbonate (PC) has long been sought after as a replacement for ethylene carbonate (EC) as the major component of the electrolyte due to the alluring physical properties of PC. [2] Specifically, PC is known to have a low very low melting point and a very high boiling point when compared to EC (reported as x-48.8°C and 36.4°C respectively) [2] which ultimately implies a greater operating range possible when using PC. However, incorporating PC into the electrolyte matrix is known to have a detrimental effect on the anode. When using PC, researchers have found that in the presence of $LiPF_6$ the electrolyte experiences continual electrolyte decomposition and no stable SEI is formed. [9,10] The continual electrolyte reduction has been shown to cause extensive graphite exfoliation and in turn eventual cell failure. [9]

In addition to the desirability of PC, the use of a different primary salt within the electrolyte matrix also has an undeniable allure. While $LiPF_6$ is a very conductive salt, it is not a very stable lithium salt. [2,11] Due to its' inherent thermal instability, LiDFOB is an attractive alternative to investigate as it is demonstrates resistance to thermal decomposition which could help with increasing the lifetime of the electrolyte which in turn will increase the life of any lithium-ion battery. Studies have been done showing that PC did work well with LiFOP as a primary salt thus it seemed prudent to try a PC based electrolyte with LiDFOB as the primary salt with the hope that comparable cycling performance could be obtain. The utilization of PC and LiDFOB is the primary focus of Chapter 2 of this dissertation and is discussed therein.

Transition Metal Dissolution Analysis from High Voltage Spinel Cathode Powder

High voltage spinel cathode material has been highly sought after within the lithium-ion battery community due to its larger operating potential. [3] However, high voltage materials also support additional concerning the materials themselves. When charged to high potentials, high voltage spinel materials are known to experience dissolution of major transition metals (specifically Mn) which ultimately causes greater problems within the lithium-ion battery cell itself. Researchers have implemented a variety of methods to overcome transition metal dissolution and ultimately improve the performance of high voltage lithium-ion battery cells with varying degrees of success reported. [14-16] Chapter 3 of this dissertation discusses our research with high voltage spinel cathode powder primarily motivated by investigating the effect crystal structure of the spinel has on transition metal dissolution.

Lithium-ion Capacitors

Lithium-ion capacitors share some similarity and stark contrast to their lithium-ion battery counterparts. In terms of construction, lithium-ion capacitors also incorporate a graphitic type anode used for lithium ion intercalation however this is where all similarities end. While the anode does experience initial lithiation, the lithiation process is solely to achieve a greater potential difference between the cathode and anode of the cell; effectively the lithiated graphite does not cycle lithium-ion in and out of the material. [17] Therefore, in theory, lithium-ion capacitors do not utilize intercalation mechanics in order to charge and discharge the cell. Instead, lithium-ion capacitors make use of an electrochemical double layer in order to facilitate charge and discharge. In order to create an electrochemical double layer, an entirely different cathode material must be used. [17]

The cathode electrode of a lithium ion capacitor is general a type of activated carbon. Unlike lithium-ion batteries, the activated carbon cathode does not allow for any intercalation mechanics to occur. Instead, an porous carbon material is used which allows for increased surface area which in turn helps to facilitate the electrochemical double layer formed to a greater extent. When current is applied, the electrolyte is solely responsible (in theory) for the charge separation seen within normal capacitors. While lithium-ion capacitors are not capable of achieving high energy densities, [17] they are quite adept at providing high rate and high power densities in comparison to lithium-ion batteries. This difference can be directly attributed to kinetics; intercalation mechanics are slow due to the fact that there are a plethora of factors that contribute to slow rate mechanics including but not limited to charge transfer mechanics, ion solvation mechanics, SEI resistance, etc. Interestingly, when working with lithium-ion capacitors, omission of intercalation mechanics allows for extremely fast charge and discharge rates. Additionally, lack of intercalation mechanics also reduces physical stress on the electrodes which directly correlates to much longer cycle lifetimes in lithium-ion capacitors. Due to the interesting opportunities lithium-ion capacitors present, Chapter 4 of this dissertation discusses out work done with lithium-ion capacitors specifically attempting to increase performance at low temperatures.

References

1. NRC (2010). Advancing the Science of Climate Change. National Research Council. The National Academies Press, Washington, DC, USA.

2. K. Xu, Chem. Rev., 104 (2004) 4303.

3. D. Linden., Handbook of Batteries, fourth ed., McGraw-Hill Professional, New York, 2010.

4. V. Etacheri, R. Maron, R. Elzari, G. Salitra, & D. Aurbach. Energy Environ. Sci., 4 (2011) 3243

5. M. Armand, J.M. Tarascon. Nature, 451 (2008) 652

6. G. Nazri, G. Pistoia., Lithium Batteries: Science and Technology, Springer Science & Business, New York, 2003.

7. R. Fong, U.V. Sacken, J. R. Dahn. J. Electochem., Soc., 137 (1990) 2009.

8. E. Peled. J. Electrochem. Soc., 126 (1979) 2047

9. A.N. Dey & B. P. Sullivan. J. Electochem. Soc., 117 (1970) 222.

10. G.C Chung, H.J Kim, S.I. Yu, S.H. Jun, J.W. Choi, M.H. Kim. J. Electrochem. Soc., 147 (2000) 4391.

11. B. Ravdel, K.M. Abraham, R. Gitzendanner, J. DiCarlo, B. Lucht, &C. Campion. J. Power Sources, 119-121 (2003) 805.

12. L. Zhou & B.L. Lucht. J. Power Sources, 205 (2012) 439.

13. D.H. Jang, Y.J. Shin, S.M. Oh, J. Electrochem. Soc., 143 (1996) 2204-2211

14. J. Cho, Y.J. Kim, T.J. Kim, B. Park. J. Electrochem. Soc., 149 (2002) A127

15. N.P.W. Pieczonka, L. Yang, M.P. Balogh, B.R. Powell, K. Chemelewski, A. Manthiram, S.A. Krachkovskiy, G.R. Goward, M. Liu. J. Phys. Chem. C, 117 (2013) 22603.

16. H. Xia, K.R. Ragavendran, J. Xie, L. Lu. J. Power Sources, 212 (2012) 28

17. B.E. Conway, Electrochemical Supercapacitors Scientific Fundamentals and Technological Applications. Kluwer Academic/Plenum Publishers, New York, 1999.

.

CHAPTER 2

Lithium Difluoro(oxalato)borate (LIDFOB) as an Alternative Salt for Propylene Carbonate Based Electrolytes

Brandon M. Knight and Brett L. Lucht

Department of Chemistry, University of Rhode Island

Kingston, Rhode Island 0288, USA

Abstract

Propylene carbonate (PC) has illustrated high level of interest as an electrolyte solvent due to have greater physical properties when compared to that of traditional ethylene carbonate (EC). Additionally, lithium difluoro(oxalate)borate (LiDFOB) has shown promise as an alternative to lithium hexafluorophosphate ($LiPF_6$) as a primary electrolyte salt. Coin cells of 1.2M LiDFOB in 3:7 PC/EMC were constructed using natural graphite/$LiCoO_2$ electrodes and cycled in order to obtain discharge capacities. *Ex situ* surface analysis of the electrodes was conducted via the use of x-ray photoelectron spectroscopy (XPS), scanning electron microscopy (SEM), and Fourier-transform infrared spectroscopy (FT-IR). The corresponding results showed that PC and LiDFOB with the addition of 1.5% vinylene carbonate cycled comparably to that of standard 1.2M $LiPF_6$ in 3:7 EC/EMC showing that LiDFOB is a good alternative salt to use in PC based electrolytes for lithium-ion batteries.

Introduction

Ethylene carbonate (EC) has been the premier component used in electrolytes for lithium-ion batteries (LIBs). [1] While highly utilized, EC doesn't have a wide range of operating temperatures due to its intrinsic physical properties. [1] In order to construct more versatile LIBs, researchers have been seeking new carbonates that have more appreciable physical properties. Propylene Carbonate was the obvious choice due it being a liquid at a wide temperature range as well as having a donor number only slightly less than that of EC. [2] However, despite the attractiveness of PC, greater complications were encountered when incorporating PC into electrolytes; specifically

extensive anode exfoliation due primarily to continuous electrolyte decomposition and failure to create a stable solid electrolyte interphase (SEI). [3-5]

Despite earlier setbacks, there have been instances in which certain our salts such as LiFOP demonstrated excellent performance when using PC. [6] Inspired by previous research hinting at the potential usefulness of lithium difluoro(oxalate)borate (LiDFOB), we attempted to investigate how LiDFOB would perform as a primary salt with a PC based solvent. However, much to our dismay, there were no appreciable capacities observed when using both PC and LiDFOB. Fortunately, research has shown that the addition of vinylene carbonate (VC) with $LiPF_6$ showed comparable performance to that of EC and $LiPF_6$ based electrolytes. [7]

Our current research focuses on investigating cells containing 1.2M LiDFOB in 3:7 PC/EMC with 1.5% VC in order to compare the performance to that of the tradition 1.2M $LiPF_6$ in 3:7 EC/EMC in order to discern how well LiDFOB is as a suitable alternative $LiPF_6$ in PC based electrolytes. Additionally, surface analysis of the electrodes post cycling provides with further information about potential electrolyte decomposition/SEI formation on the surface of the electrodes.

Experimental

Battery grade propylene carbonate (PC), ethyl methyl carbonate (EMC), ethylene carbonate, and lithium hexafluorophosphate ($LiPF_6$) were all obtained and used as received from BASF without further purification. Lithium difluoro(oxalato)borate was synthesized in lab.

Electrodes used for coin cell construction were received from MTI and consisted of natural graphite anodes and $LiCoO_2$ cathodes. Anodes were composed of 85%

natural graphite (NG), 10% conductive carbon, and 5% styrene-butadiene rubber (SBR) and carboxymethyl cellulose (CMC) pre-coated on a copper foil current collector. The cathodes were comprised of 85% $LiCoO_2$, 10% conductive carbon, and 5% PVDF pre-coated on an aluminum foil current collector. Coin cells were constructed in an argon filled glove box. Upon construction completion, coin cells were removed from Ar filled glove box and cycled from 3.0V to 4.1V on an Arbin BT4010 battery cycler at 25°C for 20 cycles. Cells were then sealed with epoxy and cycled for 10 cycles at 55°C and another 10 cycles at 25°C. The cycling profiles used for all cells consisted of one C/20 cycle, two C/10 cycles, and C/5 for all subsequent cycles. Upon cycling completion cells were disassembled within the Ar glove box, the electrodes were rinsed with dimethyl carbonate (DMC) for three washes in order to remove any residual lithium salt. The electrodes were and taken into the antechamber of the glove box and dried under vacuum overnight in preparation for the applicable surface analysis.

A JEOL 5900 Scanning Electron Microscope (SEM) was used to obtain information on the surface morphology of all electrodes. Surface chemical characterization was done using a PHI 5500 x-ray photoelectron spectrometer (XPS) set to Al Kα radiation and an aperture of 3. Processing software used for all XPS spectra was done using Multipak versions 6.1 in addition to XPS Peak 4.1 for all spectra peak fittings. Peaks were fit to the spectra using a 20% Gaussian and Lorentzian functions for the least squares curve fitting with a Shirley background. All Fourier-transform infrared spectroscopy (FT-IR) spectra were obtained using a.

Results and Discussion

Cycling Performance of Coin Cells at Room Temperature (25°C)

As illustrated by Figure 2-1, the discharge capacities observed for all three electrolyte formulations tested are very similar to each other. However, Figure 2-1 clearly indicates that the 1.2M LiDFOB in EC/EMC performed the least favorably as it shows the lowest discharge capacities of the three formulations test. This result is somewhat unexpected because EC generally facilitates lithium-ion transport better as it theoretically should bind to the lithium-ion more strongly. Interestingly, the 1.2M LiDFOB performs almost indistinguishably from the standard 1.2M $LiPF_6$ in 3:7 EC/EMC. The indication that the 1.2 LiDFOB in 3:7 PC/EMC electrolyte functions so admirably bodes well for its potential substitution for $LiPF_6$ in PC based electrolytes.

Room Temperature Resistance Measurements (25°C)

The resistance measurements shown in Figure 2-2 are also reassuring in regard to the LiDFOB/PC formulation. The resistance observed via Figure 2-2 clearly shows that the resistance seen within the 1.2M LiDFOB in 3:7 PC/EMC is well within the same resistance range as the 1.2M LiPF6 in 3:7 EC/EMC. All cells display resistances between 40Ω and 80Ω and may indicate that no unusual sources of resistance are present within any of the cells tested. This seems to indicate that all cells were constructed similarly to each other thus the cell to cell variation in this instance is minimal.

Cycling Performance of Coin Cells at Elevated Temperature (55°C)

When observing the elevated temperature cycling performance in Figure 2-3, the discharge capacities seen are also very similar to each other initially. Surprisingly, the LiDFOB/PC electrolyte deftly outmaneuvers the standard $LiPF_6$ in terms of cell

performance. The discharge capacities observed for the PC based electrolyte are indicative of greater cell performance due to the fact the discharge capacities observed remain at approximately 100 mAh/g. Based on the data witnessed herein, the PC based electrolyte certainly can withstand cycling at higher temperatures noticeably better than that of the standard 1.2M $LiPF_6$ 3:7 EC/EMC electrolyte. Interestingly, unlike most high temperature electrolytes; there appears to be no noticeable initial capacity loss when cycling at room temperature.

Elevated Temperature Resistance Measurements (55°C)

As can be seen in Figure 2-4, the resistance measurement obtained at 55°C are also consistent with the cycling data seen previously. Figure 2-4 shows that the resistance in the EC based electrolyte greatly increases in comparison to that of the PC based electrolyte. This increase in resistance correlates to the decrease in the observed discharge capacities; greater resistance implies greater impedance which in turn claim that the elevated temperature cycling of the PC based electrolyte is superior to that of the EC based electrolyte.

Coin Cell Efficiencies (25°C & 55°C)

The efficiencies obtained for all three formulations can be seen in Figure 2-5. The efficiencies show that all of the cells tested performed with approximately 99% efficiency. This seems to indicate that all the cells performed well within each formulation and any discrepancies seen can therefore be attributed to electrochemical differences between the cells with minimal cell to cell variance.

SEM Images of Anodes after Room Temperature Cycling (25°C)

The SEM images seen in Figure 2-6 appear to display very similar surface morphologies and thus there is little insight into the varied surface chemistries. Effectively they are all almost indistinguishable from each other. While minimal variances might be present within each image, none are sufficient enough draw any concise conclusions from this data.

SEM Images of Cathodes after Room Temperature Cycling (25°C)

Figure 2-7 also indicates no major difference amongst the cathodes studies which is not astonishing based on the data seen previously in regard to the anodes. The observed result is not surprising as most of the damage incurred to the surface morphologies of electrodes is traditionally seen on the anode and not the cathode. As there was no damage seen to the anodes it is also unlikely (not impossible however) that surface particle damage would be seen on the cathodes thus, this is an anticipate result.

SEM Images of Anodes after Elevated Temperature Cycling (55°C)

The SEM images of the anodes acquired in Figure 2-8 weave a very different tale than earlier samples bestowed upon us. C in Figure 2-8 clearly has different surface morphology than the fresh or that of the 1.2M $LiPF_6$ in 3:7 EC/EMC anodes. The surface of C looks as if some sort of SEI or heavy electrolyte decomposing occurred on the surface of the electrode. This result quite vexing as the PC sample which seems to vary the most in turn performed the best; one would have anticipated the anode with the most morphological abnormalities to have performed the worst. While this result is quite perplexing, it is not without merit. The bulk morphology of the 1.2M LiDFOB in 3:7 PC.EMC anode does not appear to have any major damage.

As the bulk remains unchanged, the new additions to the morphology can most likely be attributed to the formation of a type of stable SEI. While initially alarming, the increased amount of surface films on the anode is actually quite advantageous to the cycle life of the cell as witnessed by the discharge capacities seen prior. PC is well known to have difficulty forming a stable SEI when paired with graphite and which causes continual electrolyte decomposition on the surface of the anode which in turn leads to detrimental graphite exfoliation. The fact that the addition of VC (even at low concentrations) greatly enhances the PC's innate proclivity for SEI formation is truly astounding. While it is certainly possible that the film seen here might simply be heavy electrolyte reduction, the data evidenced in Figure 2-3 simply does not support that theory; if electrolyte failure occurred the results seen would not be obtainable thus the evidence strongly suggests a stable passivation layer was in fact formed.

SEM Images of Cathodes after Elevated Temperature Cycling (55°C)

The SEM Images in Figure 2-9 clearly illustrates that no significant morphological changes occurred to any of the species investigated. As previously reflected upon, it is not unusual to see no substantial changes to the cathode material under these conditions; most of the changes to the surface morphology will be observed on the anode side (if any changes occur at all). Despite the blatantly harsh cycling environment, the cathode remains unchanged.

XPS Spectra of Anodes after Room Temperature Cycling (25°C)

The XPS spectra of the anodes at room temperature give significant insight into the chemicals found on the surface of the electrodes. Figure 2-10 illustrates that there are almost certainly oxalate species from the LiDFOB present on the surface of

the anode based on the C1s spectrum observed. As the C1s spectrum of the LiDFOB with PC clearly illustrates, the oxalate peak seen between 288eV and 287.5eV. Interestingly, with the LiDFOB with EC formulation the observed peak is much larger. The discrepancy seen with the peak intensity might be correlated to electrolyte stability. The EC/LiDFOB formulation did not perform nearly as well as the PC/LiDFOB formulation as illustrated previously by the cycling performance. Due to the large amount of oxalate believed to be on the surface of the LiDFOB/PC, this may indicated that the EC based system decomposed more readily than that of the PC based electrolyte tested; this would account for the performance differences observed between the two matrices.

The F1s and O1s spectra provide minimal insight into the differences in performances observed between cells. The fluorine spectra seen of the PC and EC LiDFOB formulations clearly vary from that of the standard 1.2M $LiPF_6$ electrolyte tested. This result alludes to the fact that the SEI formed on the LiDFOB cells is different than that of the $LiPF_6$; this result is not remotely surprising. Unfortunately, the F1s and O1s spectra observed for the LiDFOB electrolytes show very little variance between each other and are effectively indistinguishable from each other. Thus, the XPS data gives us little insight into the differences between the SEI of the LiDFOB/EC and LiDFOB/PC systems.

XPS Spectra of Cathodes after Room Temperature Cycling (25°C)

The results of cathode XPS spectra obtained are most ominously disconcerting in regard to the EC/LiDFOB based electrolyte. The EC/LiDFOB electrolyte shows clear evidence of major electrolyte decomposition at room temperature. The C1s

spectrum shows a large amount of oxalate on the surface which is unusual for the cathode side of the electrode. There also appears to be what is normally attributed to LiF present within the F1s spectrum which may indicate that the LiDFOB salt itself is in fact decomposing under these conditions. Additionally, the O1s of the EC/LiDFOB system seems to have formed a film over the cathode as the metal oxide peak present in all other samples has effectively vanished. These two results are strongly indicative of electrolyte decomposition; ultimately, it appears as both the salt and solvents are degrading at a greater rate than the other formulations tested.

Aside from the EC/LiDFOB spectra observed the remaining cathode spectra leave much to be desired in terms of elucidating potential surface films present on the cathode. Figure 2-11 shows that there does appear to be a minimal surface film being formed on the surface of the cathode within the O1s spectrum of the LiDFOB/PC cathode. However, aside from noticeable diminishment of the metal oxide peak seen within the LiDFOB/PC cathode spectrum and the and increase of the peaks seen at ~534eV (most likely due to LiDFOB decomposition based on the similarity to the EC/LIDFOB spectrum seen), the PC/LiDFOB spectra vary minimally from that of the standard 1.2M $LiPF_6$ electrolyte As previously stated, there does appear to be a surface film formed on the cathode of the PC based electrolyte however the layer appears to be extremely thin as the metal oxide is still clearly present on the surface.

XPS Spectra of Anodes after Elevated Temperature Cycling (55°C)

The XPS spectra seen in Figure 2-12 tell quite an unusual tale. The C1s spectra are by far the most anomalous data encountered thus far. When comparing the C1s of The PC based electrolyte to that of the standard, it can be observed that

strangely there is no oxalate peak present in the data (at ~287.5eV) acquired. These results are particularly unsettling for a multitude of reasons. First, based on the composition of the 1.2M LiDFOB PC/EMC+1.5% VC electrolyte, the oxalato group of the LiDFOB should contribute significantly to some SEI formation. Conversely, LiDFOB is theorized to be more stable than tradition $LiPF_6$ thus it might be possible to not witness any oxalate remnants on the surface after washing the anode. However, because the SEM images clearly showed some sort of film on the surface this result seems highly improbable. Compounded by the fact studies have shown SEI formation when using PC is almost non-existent with graphite (excluding the seemingly heroic intervention of VC) leads one to believe that the LiDFOB should play some role in the SEI, even if only slightly. Even more so, due to the rigorous cycling conditions (55°C) one would expect the LiDFOB to illustrate a greater predilection towards decomposition despite its greater inherent thermal stability when compared to that of $LiPF_6$. Finally, due to the fact VC is found in very low concentrations within the system the layer observed via SEM cannot solely be due to VC either. There is no clear resolution to this discrepancy. The C1s spectra of the 1.2M $LiPF_6$ is much as it was anticipated to be as there was probably a lot of significant electrolyte reduction due to the peaks seen at ~287eV can due to the C-O bonds that are characteristic of that region. Finally, The C1s spectra do not indicate any PVDF is present within any of the spectra observed. This clearly indicates the binder used within the anode is not PVDF but a carbon/oxygen containing species.

The F1s spectrum of the fresh further corroborates the notion that PVDF is not present in the binder as there is almost no signal present. Therefore, it can be safely

concluded that no PVDF is present. Additionally, the F1s spectrum of the anode of PC based electrolyte clearly shows a very large amount of fluorine on the surface of the electrode; the only source of fluorine is the LiDFOB thus it must have decomposed on the surface. While this does nothing to further elucidate why no oxalate can be seen in the carbon spectrum, it is reassuring to know that decomposition did occur. Finally, the peak seen within the PC anode of the F1s spectrum at approximately 686.5eV are normally attributed to lithium fluorophosphates. Consequently, as there is no phosphorus in the PC based electrolyte, those species must be a reduction s of the oxalate this reinforcing the thought that the LiDFOB does contribute significantly to the SEI.

The O1s spectra obtained to relay much information about the possible reduction products present on the surface of the anodes. This is mostly due to the fact that there was an abundance of oxygen containing species seen in the fresh. However, it can be inferred that any new oxygen containing species that have arisen are most likely due to the reduction of the EC and PC on the surface of the anode.

XPS Spectra of Cathodes after Elevated Temperature Cycling (55°C)

The major area of interest with the cathode spectra obtained can be found within that of the O1s spectra, specifically the spectrum of the PC based electrolyte. As can be seen in the fresh and $LiPF_6$ spectra, the metal oxide peak s seen at 529eV is clearly present in both spectra. However, there is no metal oxide peak present within the spectrum of the cathode with the PC based electrolyte. This is clear evidence that when subjected to high temperatures the LIDFOB must be capable of creating oxidation products that form a thin film on the cathode. This is further supported by

the fact the C1s spectrum for the anode of the PC based electrolyte also clearly shows the presence of oxalate which also suggests the LiDFOB might form an oxidative film on the surface of the cathode.

Elemental Concentrations on the Surface of the Electrodes Obtained via XPS

The elemental concentrations for the anodes seen in Table 2-1further reinforce the results seen within the XPS spectra themselves. As to be expected, the carbon elemental percentage ratio decreases significantly in all cycled test samples. This is an expected result as all formulations should form an SEI on all of the anodes tested in order show any type of appreciable cycling performance. The electrolyte decomposition products contain carbon but also contain a plethora of oxygen and fluorine thus the relative ration of carbon (due to graphite) should decrease considerably upon cycling which all of the samples illustrate.

Another interesting aspect of the carbon data obtained lies within the standard $LiPF_6$ electrolyte at both 25°C and 55°C. The concentration of carbon decreases when cell is exposed to elevated temperatures. This result reveals much about electrolyte performance at elevated temperatures. Electrolyte decomposition increases as temperature increases. However, the thermal decomposition seems to include the lithium salt in addition to the normal carbonate reduction. Therefore, we see an increase in the fluorine and oxygen concentrations at the surface due to the increased reduction seen at elevated temperature this lowering the relative carbon concentration.

The LiDFOB/PC electrolyte formulation appears to remain almost unchanged when moving from 25°C to 55°C cycling. However, the doubling of the boron helps us distinguish a couple of very important morsels of information. The inclusion of

boron on the surface of the anode in appreciable concentration means that the LiDFOB is in fact a large component of SEI formation within the PC based electrolyte. Additionally, regardless of how the salt decomposes, there must be oxalate present on the surface of the electrode if boron is a component of the SEI. Therefore, this once again illustrates there is almost certainly an oxalate species present on the surface of the anode within the PC based electrolyte system. However, based on the reduction of the amount of the oxygen present may be indicative that there is a boron decomposition product forming that is independent of the oxalate species.

Finally, the EC/LiDFOB elemental concentrations on the anode seem to be telling of electrolyte instability/poor SEI formation. The oxygen content of the EC based electrolyte is 10% larger than that of the PC based electrolyte at 25°C. This result is consistent with the data seen from all other surface analysis techniques employed in these studies. The high oxygen content is most likely due to the salt/carbonates readily decomposing within the electrolyte. The excess oxygen is most likely due to an oxalate containing reduction product which is once again consistent with the other data acquired herein. Additionally, the fact that there is almost double the amount of boron on the surface of the EC anode within regard to the PC anode is quite alarming. The data shows that more boron is generated on the surface of the PC anode at elevated temperature. The fact that the same percentage is present at room temperature for the EC electrolyte does not bode well for its utilization as a $LiPF_6$ alternative electrolyte. The results seem to indicate that the LiDFOB does not pair well with EC in order to form a stable electrolyte. However, the PC electrolyte does

require VC thus the possibility exists that if VC were added to the EC based electrolyte the performance might improve significantly.

The cathode elemental concentrations seem to indicate that there may be a film formed on the surface of the cathodes especially at elevated temperature. All formulations seem to experience a greater amount of surface film on their respective cathodes as illustrated by the concentrations seen within Table 2-2. The large increase in oxygen at the surface is indicative that there may be a surface film forming on all cathodes at elevated temperature. However, the EC/LiDFOB based electrolyte cathode seems to experience reductive decomposition to a much greater extent. It appears to be evident that at room temperatures the EC based electrolyte decomposition is quite serious. The boron content on the cathode within the EC based electrolyte is almost ten times larger than the PC based electrolyte. This results fall in line with the data seen previously especially the XPS O1s spectrum of the EC electrolyte in which there was no metal oxide peak present. At this point it is clear the EC/LiDFOB based electrolyte encounters serious electrolyte stability complications when cycled at only room temperature.

FT-IR Analysis of Anodes at Room Temperature (25°C)

The FT-IR spectra obtained of the anodes do support some of the findings seen within the XPS spectra seen previously. As can be seen by Figure 2-14, as previously speculated, the binder used is most definitely not the standard PVDF as none the peaks observed. This is consistent with the data seen from the XPS. Within the standard 1.2M $LiPF_6$ electrolyte there is very little change in the spectrum within regard to the fresh aside from a rather large and broad peak at ~1500cm^{-1}. However, since the XPS

spectra obtained indicated a relatively thin SEI, the peak seen is most likely a combination of surface reduction products (lithium alkyl carbonates) and the residual binder itself. This is mostly attributed to the fact that the overall shape of the 1.2M $LiPF_6$ anode spectrum does not vary much from what can be observed from the fresh anode.

The EC/LiDFOB and PC/LiDFOB spectra clearly indicate that the SEI formed is very similar in both cases based on the spectra presented in Figure 2-14. This is not unusual as the date collected from the XPS seemed to indicate that surface of both electrodes were in fact quite similar. The intensity of the peak observed that can be attributed to the binder is greatly diminished indicating there is a thicker SEI formed for both LiDFOB derivatives. Two almost identical peaks arise at ~1650cm^{-1} and 1100cm^{-1} as well as two smaller peaks at 1450cm^{-1} and 1350cm^{-1}. Clearly these peaks seem to represent the decomposition of the LiDFOB on the surface of the electrodes. This can be inferred due to the overwhelming similarity of both the PC and EC based with LiDFOB electrolytes in contrast to the large disparity seen within regard to the standard $LiPF_6$ based electrolyte. Also, the EC/LiDFOB and EC/LiPF6 electrolytes clearly do not form a similar SEI based on the spectra obtained here as well as the spectra obtained from the XPS. These results suggest that the primary component responsible for SEI formation is not lithium ethylene dicarbonate (LEDC) within these systems which contrasts directly to that of $LiPF_6$ based electrolytes.

FT-IR Analysis of Anodes at Elevated Temperature (55°C)

The results found in Figure 2-15 are somewhat unexpected. Based on the spectra obtained, the electrolyte decomposition at elevated temperatures seems to align

more closely than at room temperature. The spectrum of the PC based electrolyte looks very similar to that of the standard. The only errant peak observed within the PC FT-IR spectrum can be seen at approximately 1650cm^{-1}. This peak is most likely due to the oxalate which in turn reinforces that there is almost definitely oxalate formed on the surface of the anode. The XPS C1s spectrum obtained for the PC based electrolyte was somewhat inconclusive as there was no noticeable oxalate peak seen which was very anomalous. However, the other spectra seemed to indicate there was in fact oxalate present and the FT-IR spectrum of the PC/LiDFOB electrolyte even also indicates there is oxalate present on the surface of the anode. This result falls in line with what was to be expected and clarifies previous discrepancies seen within the results PC anode results.

Conclusions

Based on the results acquired, 1.2M LiDFOB in 3:7 PC/EMC + 1.5% seems like an acceptable substitute for the standard 1.2M $LiPF_6$ electrolyte. The cells constructed formed indistinguishably from the standard $LiPF_6$ electrolyte and retained greater stability after cycling at elevated temperature. This result is somewhat miraculous considering PC/EMC without VC will not cycle in the slightest. The addition of a minimal amount of VC seems to indicate that it must be conducive to stable SEI formation within PC based electrolytes. The problems encountered with LiDFOB and EC may in fact be very similar to the problems originally encountered with PC when not using VC. Thus, the next logical step would be to compare the performance of the EC electrolyte with VC to see if it in fact surpasses the PC based electrolyte in performance.

The surface analysis results seem to indicate that oxalate is a prominent player in the SEI formation as well as boron. The major complications facing the EC based electrolyte seem to be related to electrolyte stability with EC thus the VC addition in the PC based electrolyte almost certainly assists in SEI stability and allows good electrolyte passivation to occur.

Acknowledgement

This research project was funded by DoE EPSCoR. All the work carried out here was completed at the University of Rhode Island

References

1. D. Linden., Handbook of Batteries, fourth ed., McGraw-Hill Professional, New York, 2010.

2. K. Xu, Chem. Rev., 104 (2004) 4303.

3. A.N. Dey & B. P. Sullivan. J. Electrochem. Soc., 117 (1970) 222.

4. G.C Chung, H.J Kim, S.I. Yu, S.H. Jun, J.W. Choi, M.H. Kim. J. Electrochem. Soc., 147 (2000) 4391.

5. R. Fong, U.V. Sacken, & J. R. Dahn. J. Electrochem., Soc. 137 (1990) 2009.

6. L. Zhou & B.L. Lucht. J. Power Sources, 205 (2012) 439.

7. C.C. Chang, S.H. Hsu, Y.F. Jung, C.H. Yang. J. Power Sources, 196 (2011) 9605.

.

Table 2-1: Elemental Concentration Present on the Surface of the Anode Calculated via XPS

Anode Elemental Concentrations via XPS (%)					
Sample	C1s	F1s	O1s	P2p	B1s
Fresh	80	0	20	---	---
$LiPF_6$ (55°C)	40	24	33	3	---
LiDFOB (PC; 55°C)	47	14	29	---	10
$LiPF_6$ (25°C)	49	20	30	1	---
LiDFOB (PC; 25°C)	46	16	34	---	4
LiDFOB (EC; 25°C)	36	14	41	---	9

Table 2-2: Elemental Concentrations at the Surface of the Cathode Calculated via XPS

Cathode Elemental Concentrations via XPS (%)						
Sample	C1s	F1s	O1s	P2p	B1s	Co2p
Fresh	69	22	8	---	---	1
$LiPF_6$ (55°C)	54	28	16	1	---	1
LiDFOB (PC; 55°C)	42	21	28	---	9	0
$LiPF_6$ (25°C)	73	15	10	0	---	2
LiDFOB (PC; 25°C)	57	21	19	---	1	2
LiDFOB (EC; 25°C)	45	20	29	---	5	2

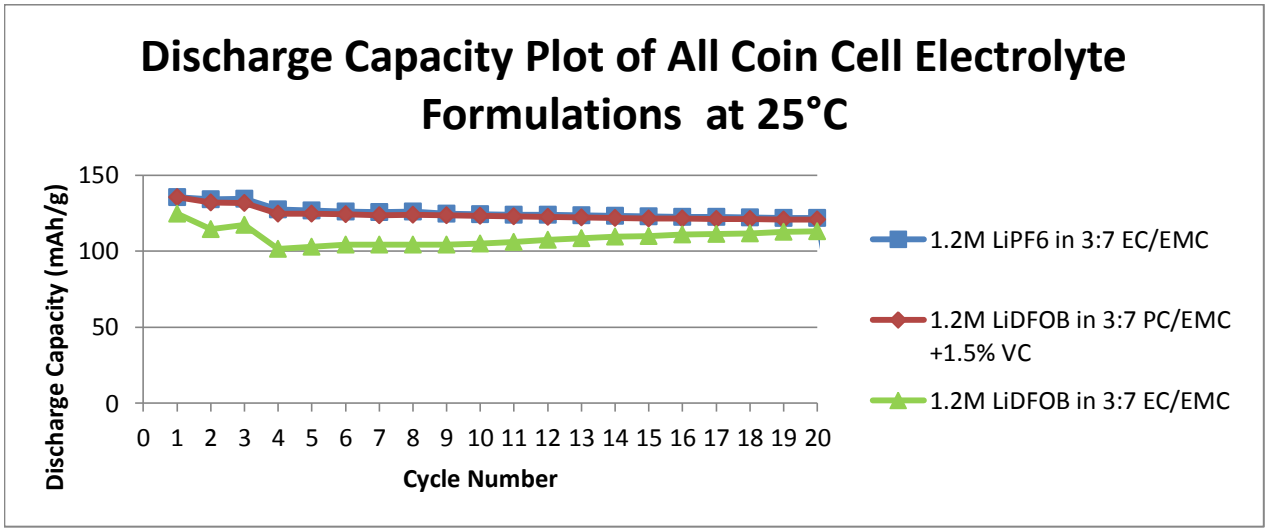

Figure 2-1: Discharge Capacities of 1.2M $LiPF_6$ in 3:7 EC/EMC, 1.2M LiDFOB in 3:7 PC/EMC + 1.5% VC (wt.), and 1.2M LiDFOB in 3:7 EC/EMC after Cycling at Room Temperature (25°C)

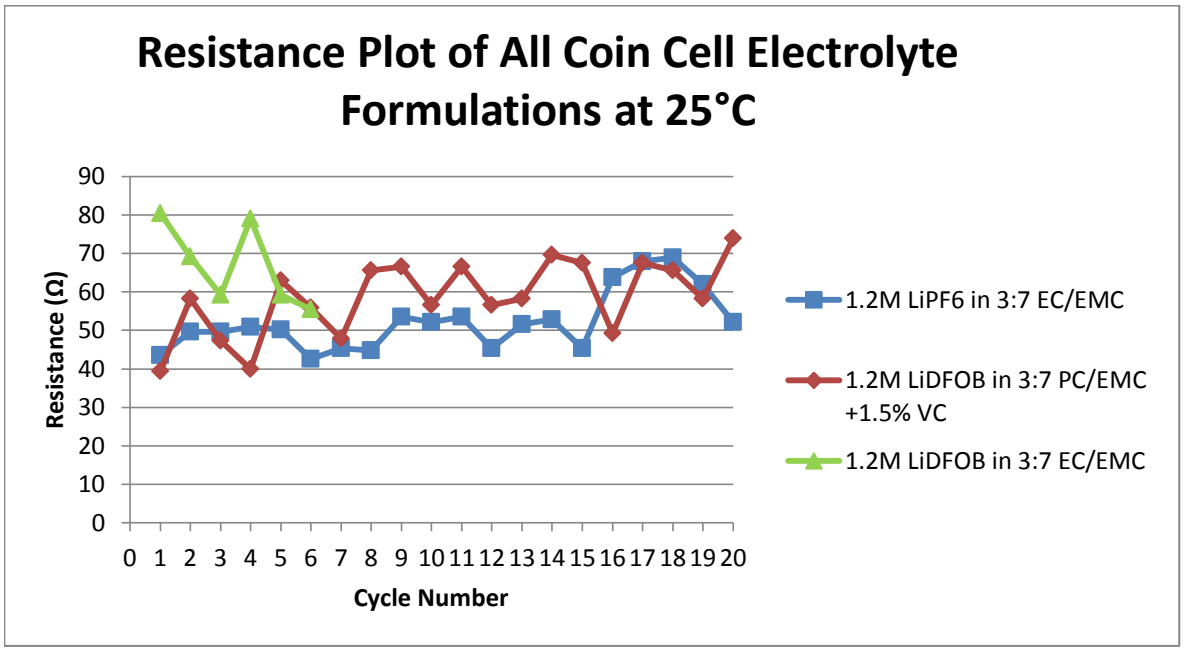

Figure 2-2: Resistances of 1.2M $LiPF_6$ in 3:7 EC/EMC, 1.2M LiDFOB in 3:7 PC/EMC + 1.5% VC (wt.), and 1.2M LiDFOB in 3:7 EC/EMC after Cycling at Room Temperature (25°C)

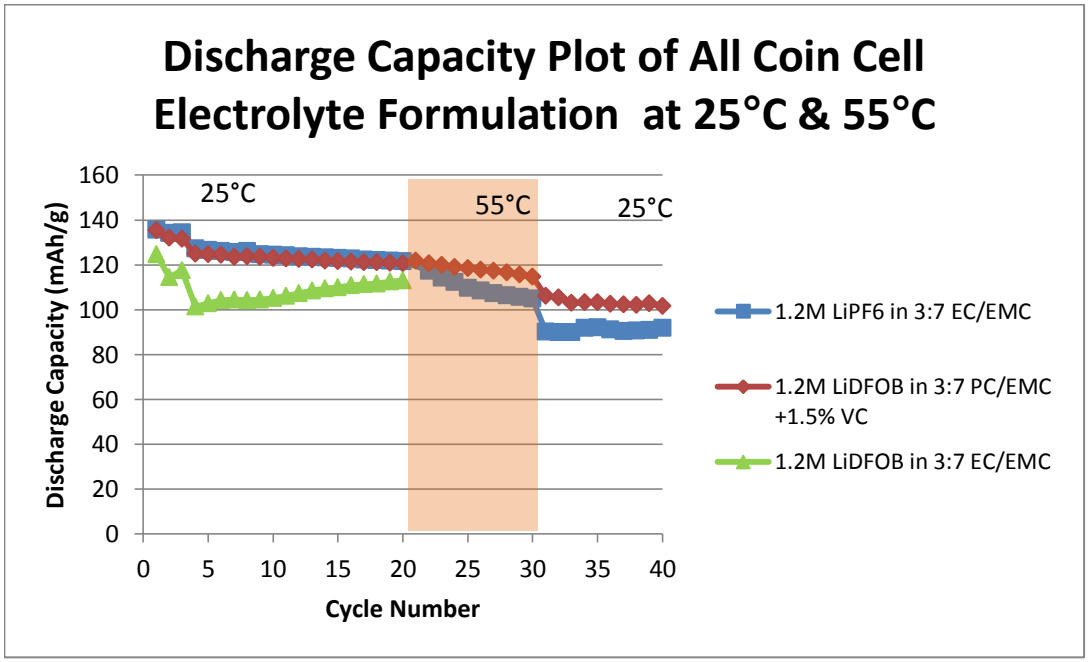

Figure 2-3:Discharge Capacities of 1.2M $LiPF_6$ in 3:7 EC/EMC, 1.2M LiDFOB in 3:7 PC/EMC + 1.5% VC (wt.), and 1.2M LiDFOB in 3:7 EC/EMC after Cycling at 25°C and 55°C

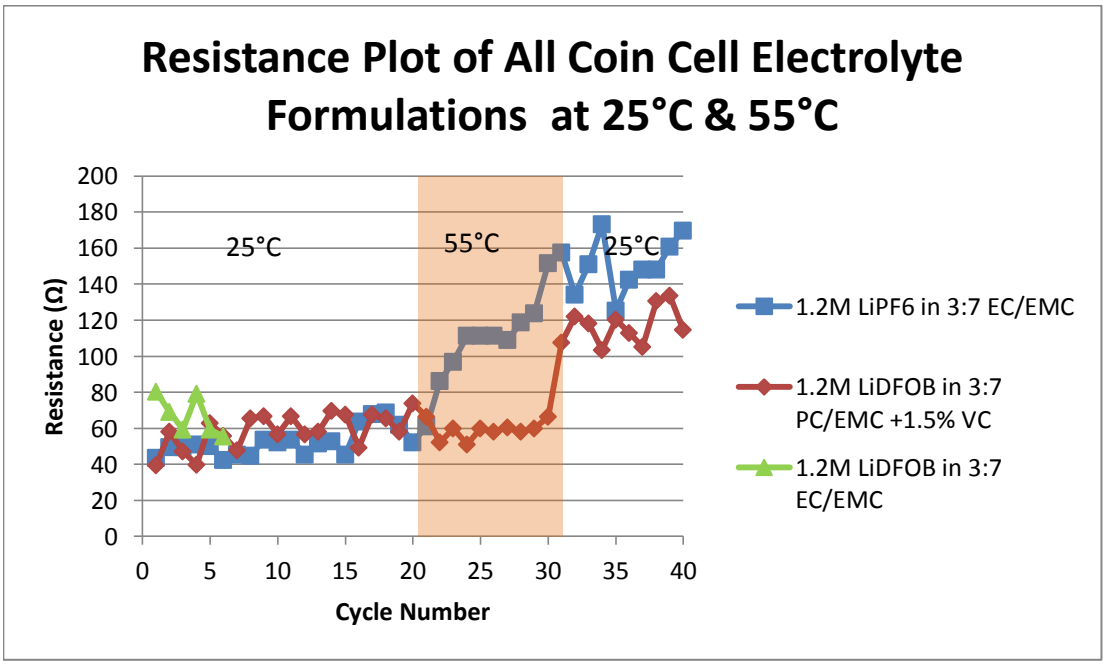

Figure 2-4:Resistances of 1.2M $LiPF_6$ in 3:7 EC/EMC, 1.2M LiDFOB in 3:7 PC/EMC + 1.5% VC (wt.), and 1.2M LiDFOB in 3:7 EC/EMC after Cycling at 25°C and 55°C

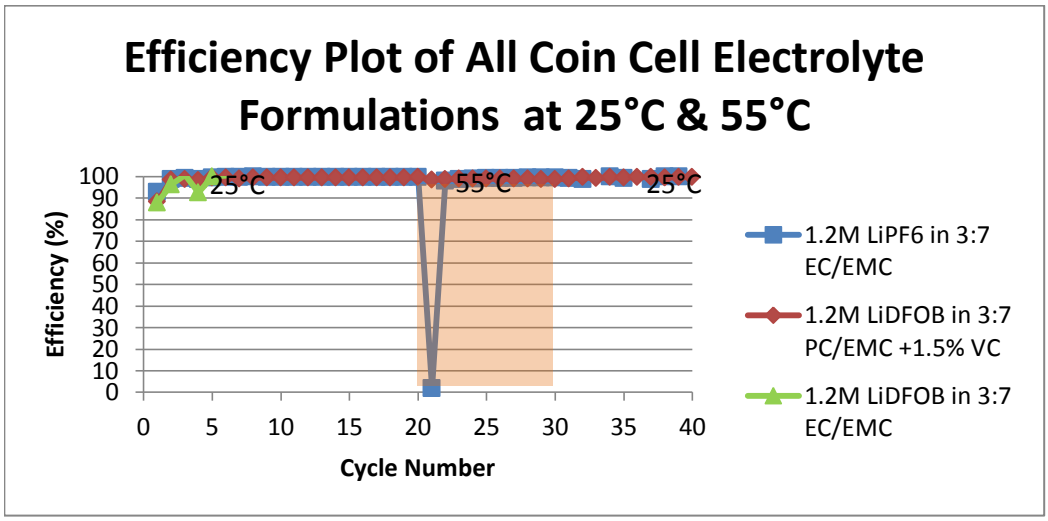

Figure 2-5: Efficiencies of 1.2M $LiPF_6$ in 3:7 EC/EMC, 1.2M LiDFOB in 3:7 PC/EMC + 1.5% VC (wt.), and 1.2M LiDFOB in 3:7 EC/EMC after Cycling at Room Temperature (25°C) and Elevated Temperature (55°C).

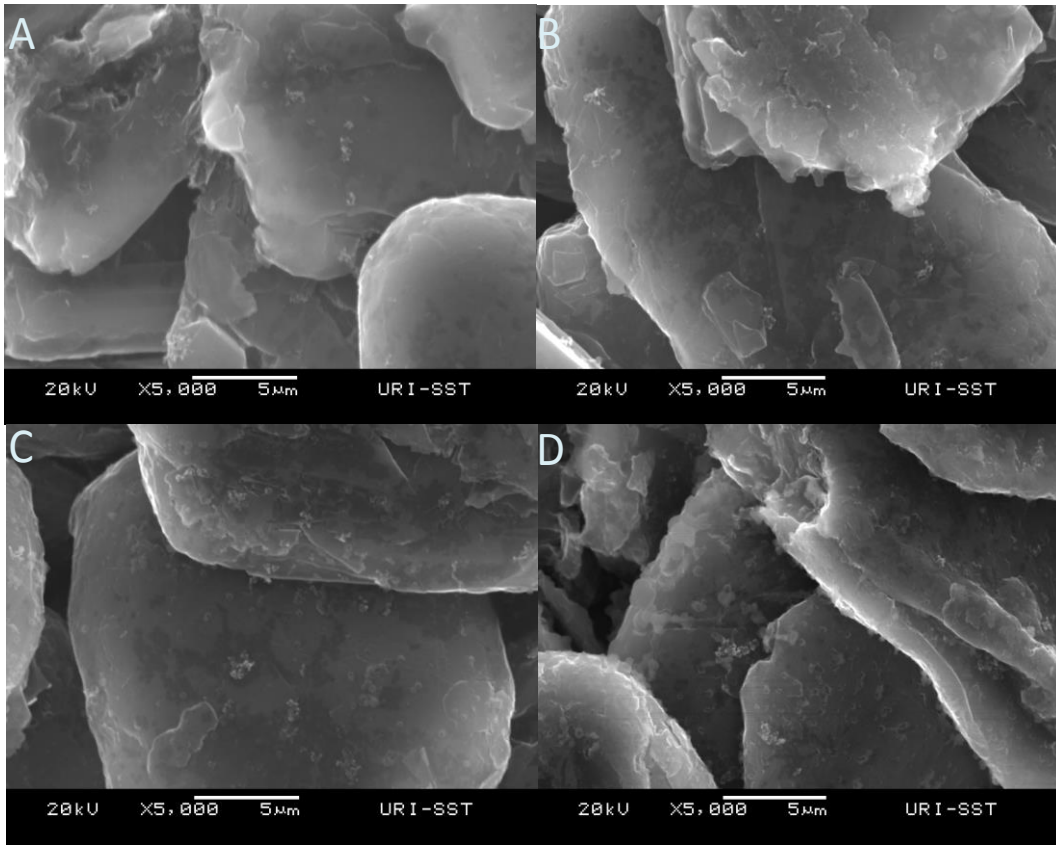

Figure 2-6: SEM Images of MTI Anodes after Room Temperature Cycling (25°C). A) Fresh Cathode; B) 1.2M $LiPF_6$ in 3:7 EC/EMC; C) 1.2M LiDFOB in 3:7 PC/EMC +1.5% VC (wt.); D) 1.2M LiDFOB in 3:7 EC/EMC.

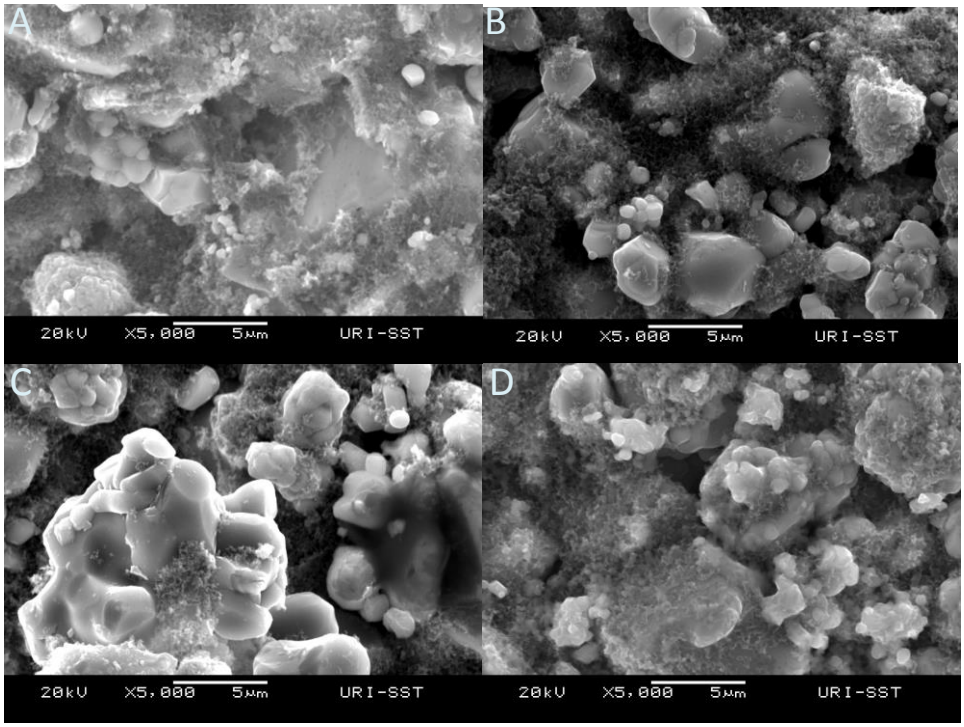

Figure 2-7: SEM Images of MTI Cathodes after Room Temperature Cycling (25°C). A) Fresh Cathode; B) 1.2M $LiPF_6$ in 3:7 EC/EMC; C) 1.2M LiDFOB in 3:7 PC/EMC +1.5% VC (wt.); D) 1.2M LiDFOB in 3:7 EC/EMC.

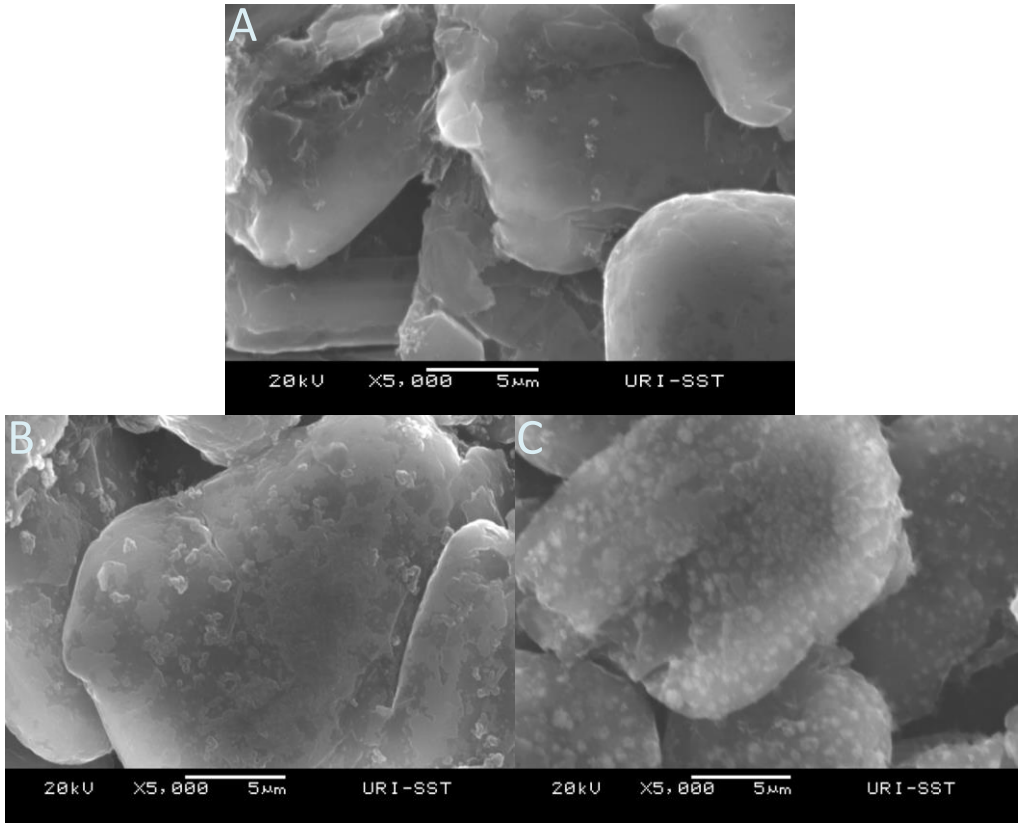

Figure 2-8: SEM Images of MTI Natural Graphite Anodes after Cycling at Elevated Temperature (55°C). A) Fresh Anode; B) 1.2M $LiPF_6$ in 3:7 EC/EMC; C) 1.2M LiDFOB in 3:7 PC/EMC +1.5% VC (wt.)

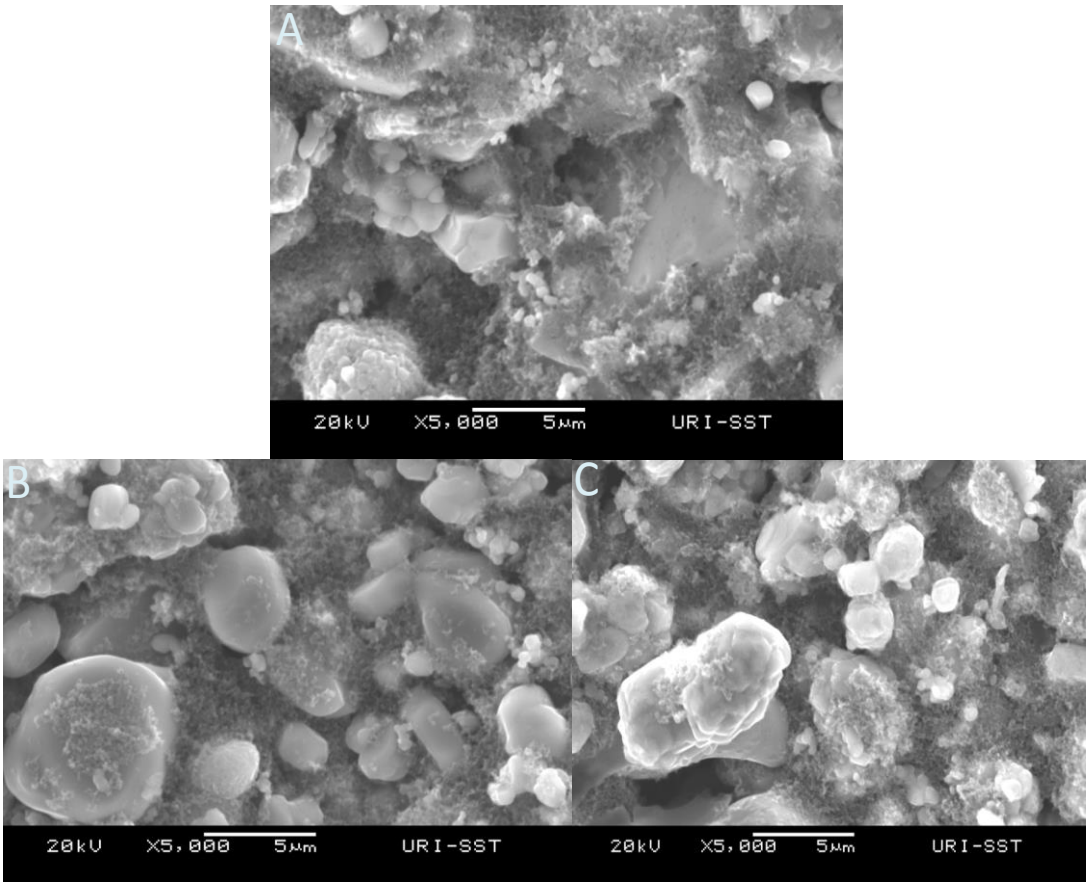

Figure 2-9: SEM Images of MTI $LiCoO_2$ Cathodes after Elevated Temperature Cycling (55°C). A) Fresh Cathode; B) 1.2M $LiPF_6$ in 3:7 EC/EMC Cathode; C) 1.2M LiDFOB in 3:7 PC/EMC + 1.5% VC (wt.).

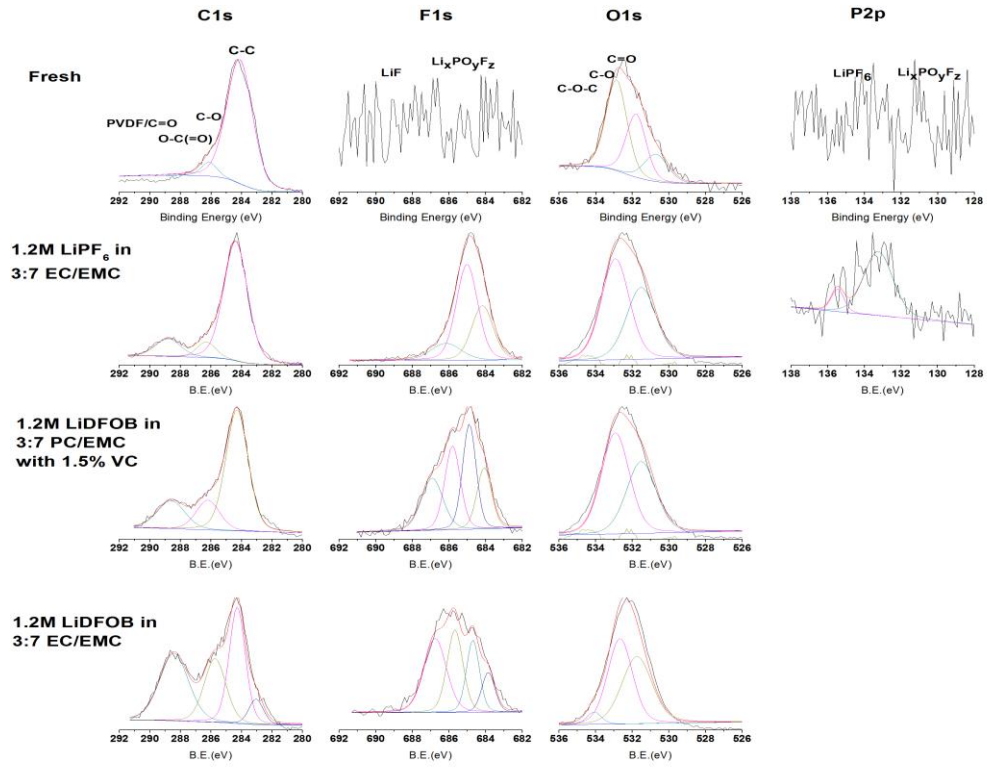

Figure 2-10: XPS Spectra of Fresh, 1.2M $LiPF_6$ in 3:7 EC/EMC, 1.2M LiDFOB in 3:7 PC/EMC Anodes and 1.2M LiDFOB in 3:7 EC/EMC After Room Temperature Cycling (25°C)

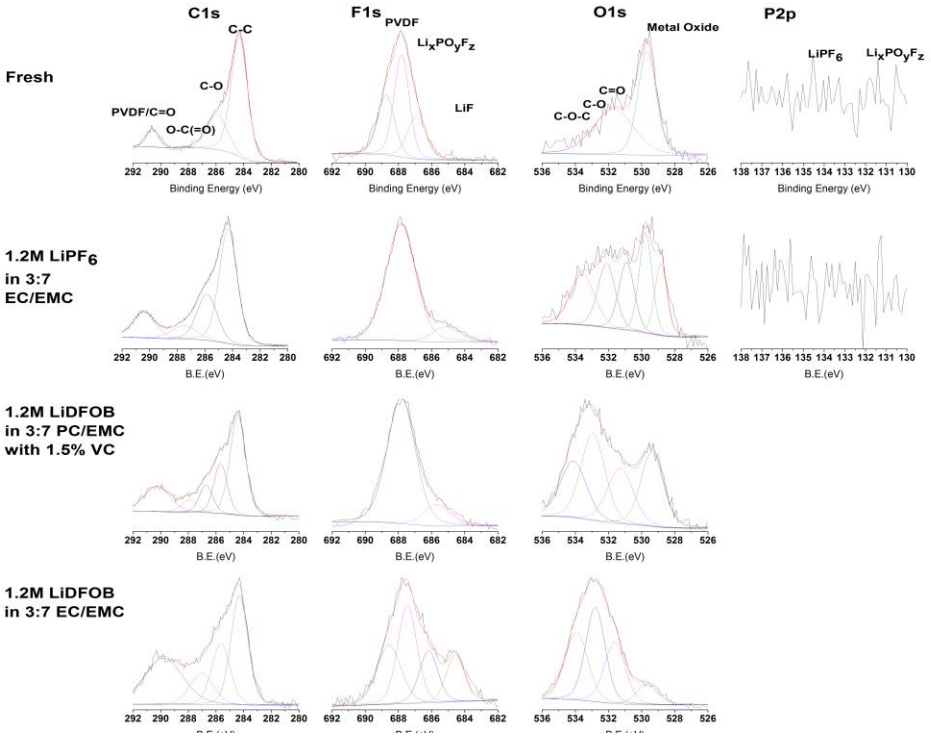

Figure 2-11: XPS Spectra of Fresh, 1.2M $LiPF_6$ in 3:7 EC/EMC, 1.2M LiDFOB in 3:7 PC/EMC, and 1.2M LIDFOB in 3:7 EC/EMC Cathodes after Room Temperature Cycling (25°C).

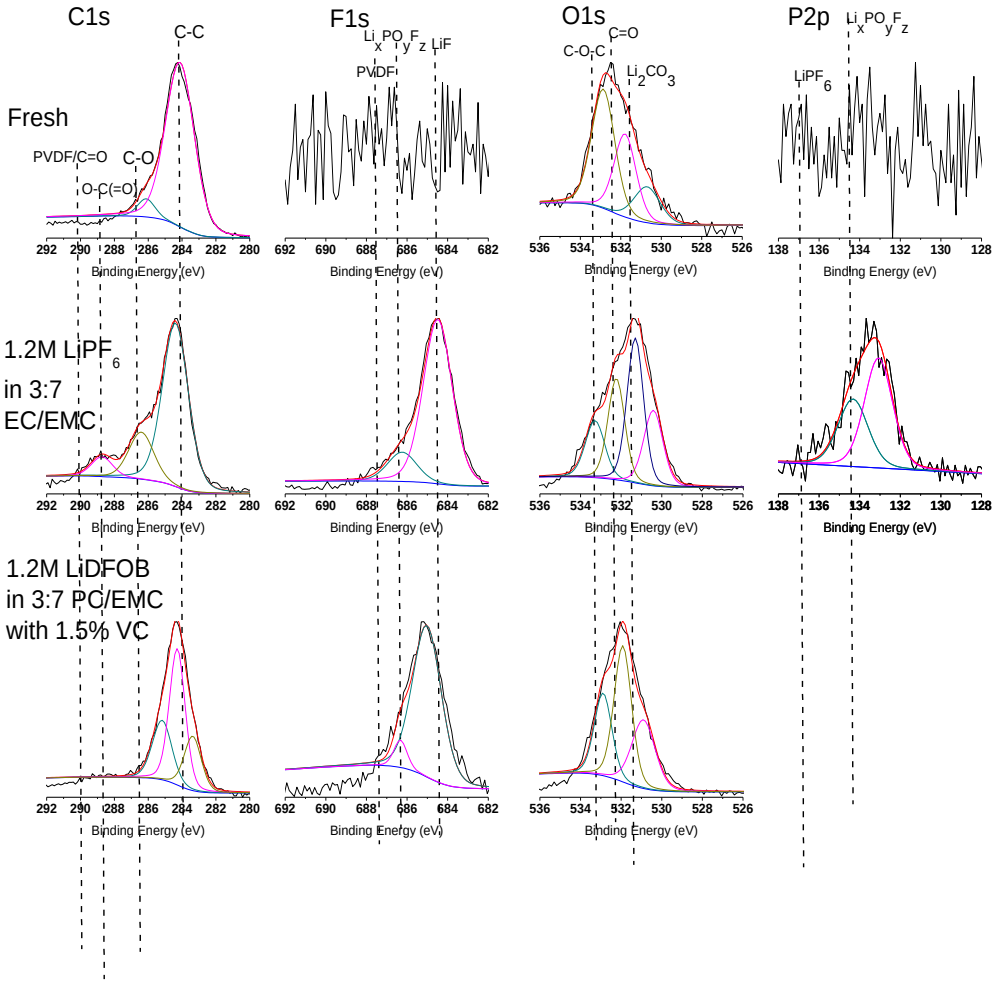

Figure 2-12: XPS Spectra of Fresh, 1.2M $LiPF_6$ in 3:7 EC/EMC, and 1.2M LiDFOB in 3:7 PC/EMC Anodes After Elevated Temperature Cycling (55°C)

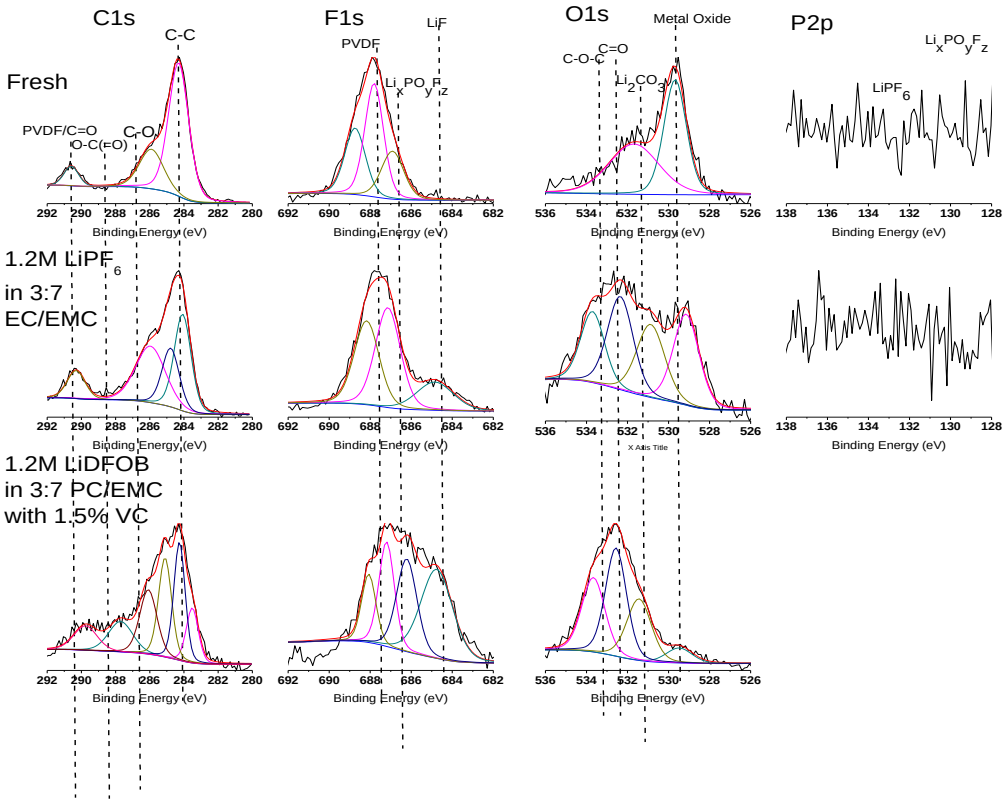

Figure 2-13: XPS Spectra of Fresh, 1.2M $LiPF_6$ in 3:7 EC/EMC, and 1.2M LiDFOB in 3:7 PC/EMC Cathodes after Elevated Temperature Cycling (55°C).

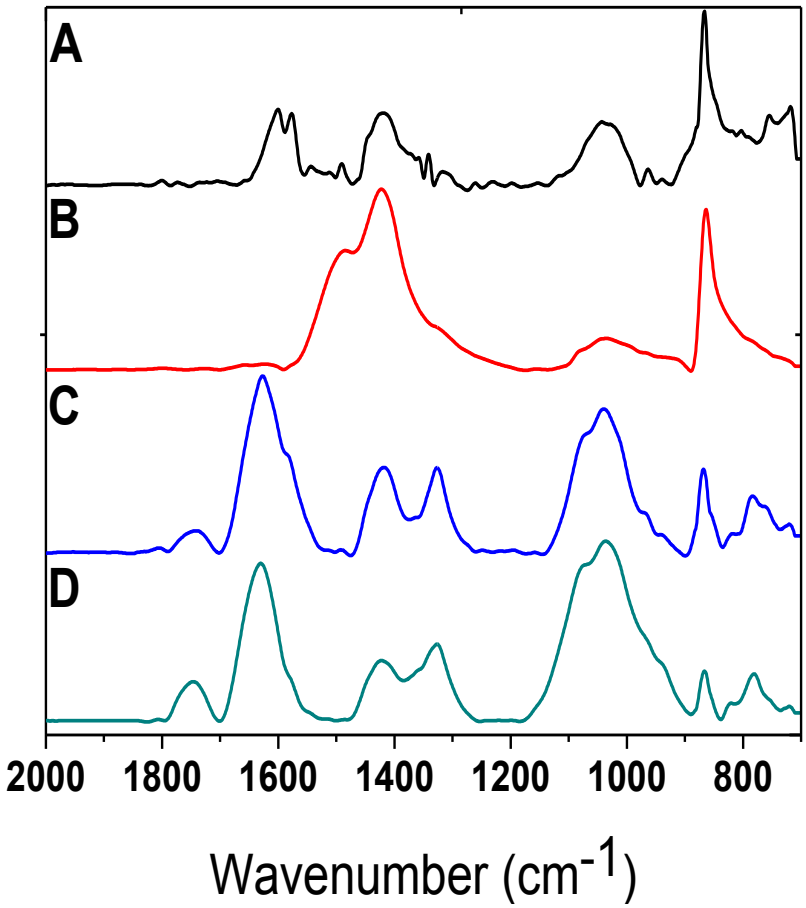

Figure 2-14: FT-IR Spectra of (A)Fresh MTI Anode, (B) 1.2M $LiPF_6$ in 3:7 EC/EMC Anode, (C) 1.2M LiDFOB in 3:7 PC/EMC + 1.5% VC Anode, (D) 1.2M LIDFOB in 3:7 EC/EMC Anode After Room Temperature Cycling (25°C).

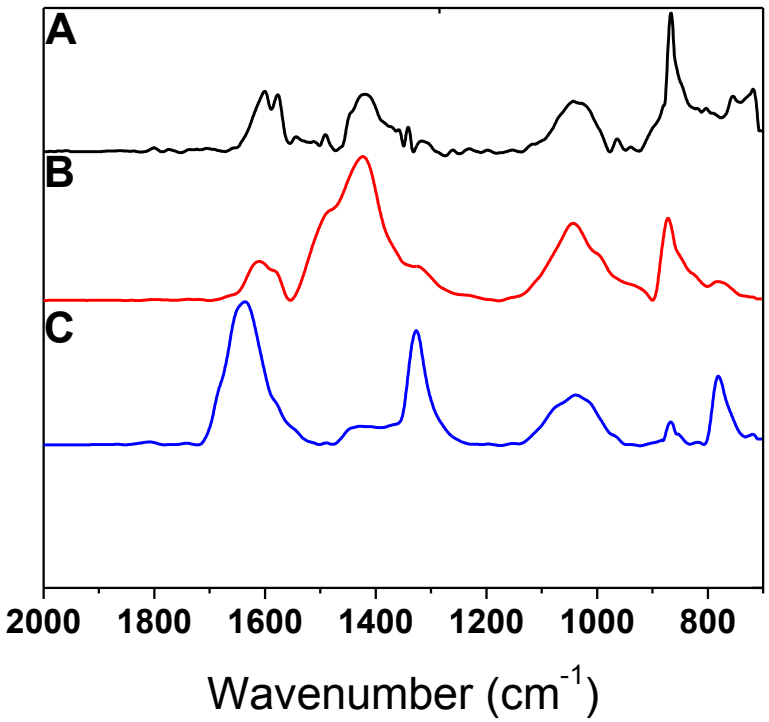

Figure 0-15: FT-IR Spectra of (A)Fresh MTI Anode, (B) 1.2M $LiPF_6$ in 3:7 EC/EMC Anode, and (C) 1.2M LiDFOB in 3:7 PC/EMC + 1.5% VC Anode After Elevated Temperature Cycling (55°C).

CHAPTER 3

TRANSITION METAL DISSOLUTION ANALYSIS FROM HIGH VOLTAGE SPINEL CATHODE POWDER VIA XPS

Brandon M. Knight[1]1, Hugues Duncan[2]2, Guoying Chen[2]2, and Brett L. Lucht[1]

[1]*University of Rhode Island, Kingston, RI 02881*

[2]*Lawrence Berkeley National Laboratory, Berkeley, CA 94720*

Abstract

The degradation of lithium manganese spinel electrodes, including $LiNi_{0.5}Mn_{1.5}O_4$, is an area of great concern within the field of lithium ion batteries (LIBs). Manganese containing cathode materials frequently have problems associated with Mn dissolution which significantly reduces the cycle life of LIB. Thus the stability of the cathode material is paramount to the performance of Mn spinel cathode materials in LIBs. In an effort to gain a better understanding of the stability of $LiNi_{0.5}Mn_{1.5}O_4$ in common $LiPF_6$/carbonate electrolytes, samples were stored at elevated temperature in the presence of electrolyte. Then after storage both the electrolyte solution and uncharged cathode particles were analyzed. The solid cathode particles were analyzed via scanning electron microscopy (SEM) whereas the electrolyte solution was analyzed using inductively coupled plasma mass spectroscopy (ICP-MS). The SEM analysis assists with elucidation of changes to the surfaces of the cathode particles. The ICP-MS of the electrolyte allows the determination of the extent of Mn and Ni dissolution. Samples of $LiNi_{0.5}Mn_{1.5}O_4$ with different crystal surface facets were prepared to investigate the role of particle morphology in Mn and Ni dissolution. The factors affecting Mn and Ni dissolution and methods to inhibit dissolution will be discussed.

Introduction

High voltage spinel type cathodes have been a greatly sought resource for its inherent higher potential window and thus greater achievable capacities than the standard lithium metal oxide cathodes traditionally used. [1] While high voltage cathodes may superficially look like the obvious choice for an electrode, further investigation reveals that high voltage materials are not without their own limitations. Transition metals from the crystal structure of the spinel have been known to dissolute from the crystal structure [2] and potentially cause damage to the anode side of the cathode decreased cell performance or failure. [3] In order to overcome these shortcomings, researchers have investigated ways to limit transition metal dissolution from the bulk material [4-5], specifically in regard to the altering the crystal structure spinel material. [6]

High voltage spinel is host to a plethora of $LiMnO_4$ type derivatives that make up the material. [1] Thus, due to the variability available to constructing spinel-like structures implies and altered crystal structure can be implemented. By changing the crystal structure researchers hope to help end the tyranny of transition metal dissolution and preserve a more stable lithium-ion battery system that can sustain higher potentials.

Our research interests lie with the investigation of the octahedral and plate crystal structures of $LiNi_{0.5}Mn_{1.5}O_4$ high voltage spinel. In order to determine whether or not crystal structure and/or ordering within that crystal structure has an overall effect on the amount of transition metal dissolution observed, ICP-MS will be used. In addition the ICP-MS, SEM will be used in an attempt to further elucidate changes

within the morphology that may help to confirm the superiority of one crystal structure over the other.

Experimental

High voltage spinel powder samples were obtained from LBL and brought into an Ar filled glove box for storage. 1.2M $LiPF_6$ in 3:7 EC/EMC electrolyte was received from BASF, stored under argon, and used as received. 30mg of spinel powder was put into an ampoule and then had 2ml of 1.2M $LiPF_6$ in3:7 EC/EMC and subsequently the ampoules were sealed with septa. Ampoules were removed from the argon glove box and taken to a schlenk line for flame sealing. The inside of the ampoules were purged with nitrogen gas and, while on the schlenk line, partial vacuum was pulled within the ampoule. A torch was then used to melt the glass neck of the ampoules in order to ensure no air or water contamination could occur. The ampoules were then place in an oil bath of 85°C for 6 days for thermal storage. Upon thermal storage completion, the ampoules were taken into the glove box, cracked, and 1mL of electrolyte was extracted and placed into a recently dried vial for further analysis. The electrolyte was removed from the glove box and heated on a hot plate within a hood in order to boil off the remaining organic solutions. Once dry, 2mL of a 3% nitric acid solution were added to the remaining polymer within each vial. Once completely dissolved, 1mL of the remaining solution was obtained from each vial and diluted to 10mL. These 10mL samples were then taken to the ICP-MS for analysis. In addition to the electrolyte the powder within the ampoules was also taken, rinsed 3 times with DMC and dried overnight within the antechamber under vacuum in preparation for SEM analysis.

Results and Discussion

ICP-MS Analysis of Electrolyte

The powder samples with the ordered plate crystals 112 facets and the samples with the octahedral crystals with 111 facets were taken to ICP-MS for analysis. The results of the ICP-MS analysis can be seen In Table 3-1. Based on the percent of transition metal dissolution the less ordered octahedral crystal structure experienced the least amount of transition metal dissolution. Interestingly, in both cases the less ordered crystal structure for both the plate and octahedral crystals experienced less transition metal dissolution which seems to indicate that ales ordered spinel crystal structure is more appreciable to being used when cycling at high voltages due solely to the face that it is more resistance to transition metal dissolution.

SEM Analysis of High Voltage Spinel Powder

SEM analysis of the high voltage spinel powder provided little insight into which of the two crystal forms retained the integrity of their morphology the best. The fresh samples are essentially indistinguishable from the powder that underwent thermal storage. As can be clearly seen in Figure 3-1 and 3-2, not surface damage can be observed despite the harsh storage conditions each of the samples experienced. This result is not very surprising considering the minimal extent of transition metal dissolution; all samples experienced less than 0.5% loss of mass as evidenced by the ICP-MS results. Therefore, since a minimal amount of transition s lost as compared to the whole, very no differences to the surface can be seen with a traditional SEM; if any damage were to be one would need a more powerful SEM in order to increase the magnification sufficiently to see small details.

Conclusions

Based on the data found herein there is not much to reinforce the assertions made by the ICP-MS results. While the results do suggest that a less ordered structure is conducive to minimizing transition metal dissolution from the cathode. However, since these results are not reflected in the SEM data, they should be regarded with the appropriate level of skepticism.

Acknowledgement

This research project was funded by DoE EPSCoR. All the work carried out here was completed at the University of Rhode Island.

References

1. D. Linden., Handbook of Batteries, fourth ed., McGraw-Hill Professional, New York, 2010.

2. D.H. Jang, Y.J. Shin, S.M. Oh, J. Electrochem. Soc. 143 (1996) 2204-2211.

3. N.P.W. Pieczonka, Z. Liu, P. Lu, K. L. Olson, J. Moote, B.R. Powell, J.H. Kim. J. Phys. Chem. C, 117 (2013) 15947

4. J. Cho, Y.J. Kim, T.J. Kim, B. Park. J. Electrochem. Soc., 149 (2002) A127

5. N.P.W. Pieczonka, L. Yang, M.P. Balogh, B.R. Powell, K. Chemelewski, A. Manthiram, S.A. Krachkovskiy, G.R. Goward, M. Liu. J. Phys. Chem. C, 117 (2013) 22603.

6. K.R. Chemelewski, E.S. Lee, W. Li, A. Manthiram. Chem. Mater., 25 (2013) 2890

.

Table 3-1: Transition Metal Dissolution Percentages via ICP-MS.

Sample	[Mn] (ppb)	[Ni] (ppb)	Mn Dissolution %	Ni Dissolution %
less ordered plate crystals with (112) facets	7277	1367	0.24	0.05
more ordered plate crystals with (112) facets	12082	2093	0.40	0.07
more ordered octahedral crystals with (111) facets	8504	2582	0.28	0.09
less ordered octahedral crystals with (111) facets	3426	974	0.11	0.03

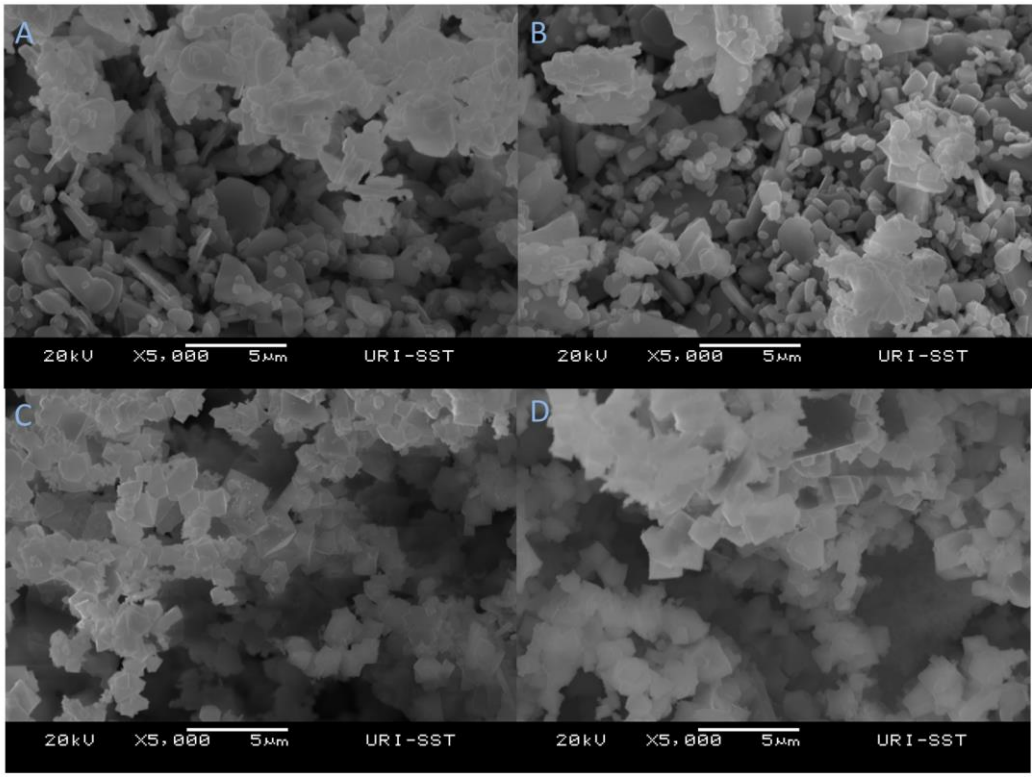

Figure 3-1: SEM Images of $LiNi_{0.5}Mn_{1.5}0_4$ from Lawrence Berkley National Labs before Thermal Storage. A) 1113 - less ordered plate crystals with (112) facets; B) 1113A - more ordered plate crystals with (112) facets; C 1115B - more ordered octahedral crystals with (111) facets; D) 1115BA - less ordered octahedral crystals with (111) facets

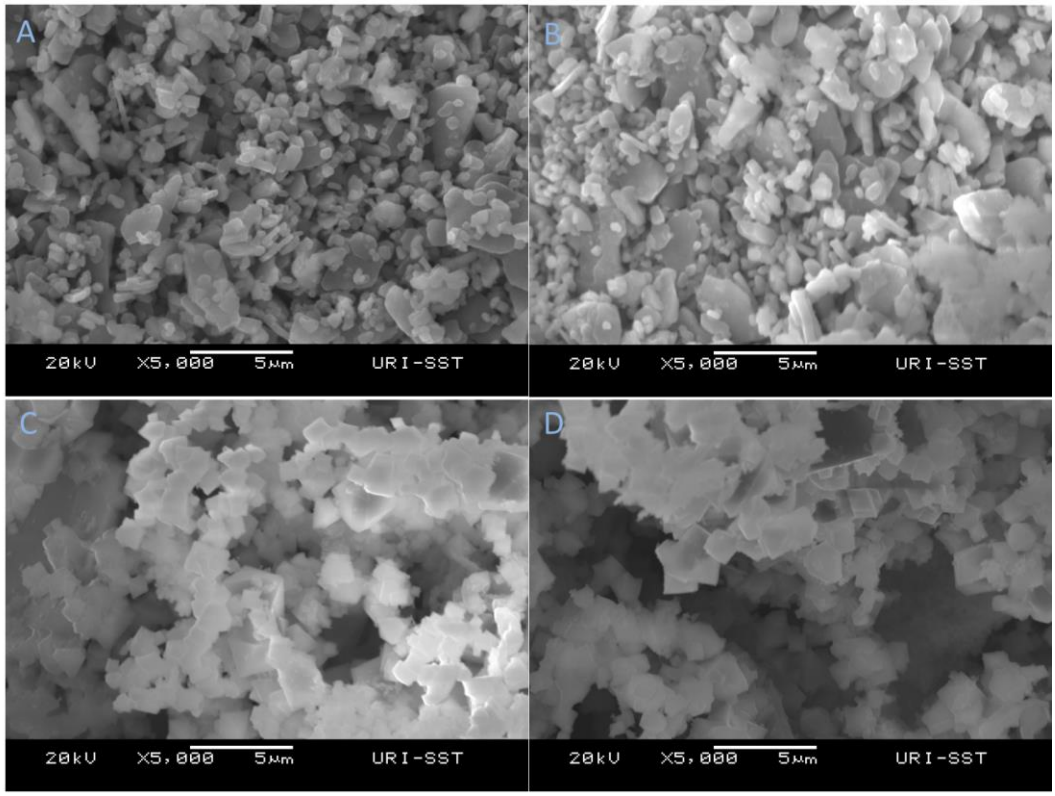

Figure 3-2: SEM Images of $LiNi_{0.5}Mn_{1.5}0_4$ from Lawrence Berkley National Labs after Thermal Storage. A) 1113 - less ordered plate crystals with (112) facets; B) 1113A - more ordered plate crystals with (112) facets; C) 1115B - more ordered octahedral crystals with octahedral crystals with (111) facets; D) 1115BA - less ordered octahedral crystals with (111) facets

CHAPTER 4

Low Temperature Performance of Lithium-Ion Capacitors

This chapter has been removed due to confidentiality agreements with Maxwell Technologies, for whom this research was completed. This chapter was successfully incorporated into the PhD dissertation defense but cannot be published